Optimal Harvesting with Autonomous Tow Vessels for Offshore Macroalgae Farming

M.S. Bhabra[*,1], M.M. Doshi[*,1], B.C. Koenig[*,1], P.J. Haley[1], C. Mirabito[1],
P. F. J. Lermusiaux[†,1], C.A. Goudey[2], J. Curcio[2], D. Manganelli[2], H. Goudey[2]
[1]*Department of Mechanical Engineering, Massachusetts Institute of Technology, Cambridge, MA*
[2]*C. A. Goudey and Associates, Newburyport, MA*
[†]Corresponding Author: pierrel@mit.edu

***Abstract*—The rising popularity of aquaculture has led to increased research in offshore algae farming. Central to the efficient operation of such farms is the need for (i) accurate models of the dynamic ocean environment including macroalgae ecosystem dynamics and (ii) intelligent path planning algorithms for autonomous vessels that optimally manage and harvest the algae fields. In this work, we address both these challenges. We first integrate our modeling system of the ocean environment with a model for forecasting the growth and decay of algae fields. These fields are then input into our exact optimal path planning, augmented with the optimal harvesting goals and solved using level set methods. The resulting path is a provable time-optimal route for the vehicle to follow under the constraint of having to monitor or harvest a specified amount of the field to collect. To demonstrate the theory, we simulate algal growth in both idealized and realistic data-assimilative dynamic ocean environments and compute the optimal paths for an autonomous collection vehicle. We demonstrate that our theory and schemes can be used to compute the optimal path in a variety of scenarios – harvesting in the case of discrete farms, a large kelp farm field, or large scale dynamic algal bloom fields.**

***Index Terms*—algae models, path planning, optimal harvesting, offshore farming, aquaculture, ocean dynamics**

I. Introduction

Offshore farming has, in the past few decades, started to gain increasing popularity. Falling under the broad field of aquaculture, these farms have typically included various different species including fish, crustaceans and aquatic plants [54]. Recently, algae has started to receive more attention as an option for aquatic farming, as research from scientists show the many possible applications of this organism in food, fodder, medicine, bio fuel and even environmental purification [29].

A key determinant, however, for the future success of algae farming as an industry is the ability to substitute traditional low-tech and labor-intensive tools and methods with automation and technology-driven solutions. Autonomous underwater and surface vehicles, which have been gaining prevalence in numerous marine applications such as naval security, scientific exploration and ocean mapping, have started to also be considered in the aquafarming industry. The use of unmanned vessels, or autonomous ocean tractors, can provide high towing efficiency while simultaneously significantly lowering the cost of operation [7].

Central to the optimal control of these autonomous vessels for efficient offshore macroalgae farming are two key components: ocean forecasting and route planning. Specifically, there is a need for accurate prediction of the (i) dynamic ocean environment including physical transports and macroalgae ecosystem dynamics, and (ii) paths of the autonomous vessels that optimally manage and harvest the algae. The dynamic effects of the ocean environment on both the algae and the relatively slow vessels are major differences with respect to classic farming on land. In this work, we address these two components and develop theory and schemes for exact optimal harvesting of algae fields using autonomous tow vessels. Our applications showcase the collection of free-flowing algae as well as of fixed or enclosed algae fields.

Path planning, in the general sense, corresponds to a set of rules to be provided to an autonomous robot for navigation from one configuration to another in some optimal fashion [48]. The metric for optimality, moreover, is problem dependent and varies with the user specified objectives and can include minimizing travel time, minimizing energy use, or maximizing vehicle safety. Numerous approaches have been studied to tackle such problems including graph search schemes such as the A^* algorithm [8], [19], [57], rapidly-exploring random trees (RRTs) [34], [37], artificial potential field methods [3], [70] and fast marching schemes [63]. Increasingly, as autonomous vehicles can be used to collect and harvest external fields from the environment – such as in offshore farming or cleaning operations – new questions must be answered. They include what governs and how to compute time-optimal paths under the constraint of collecting a certain amount of a given field prior to reaching the destination. Solving such problems requires augmenting the tried and tested, or developing completely new, path planning theory.

Successful harvesting of algae requires knowledge of how algae grows in response to various environmental parameters in order to efficiently inform the path planning collection vehicles. Algae characterization efforts have resulted in a wide variety of models that account for various strains, conditions, and biological pathways for algae growth. The bulk of these models include a handful of key algal growth parameters including light, temperature, and nutrients [12]. Many models describe algae growth in very specific farm conditions, and thus assume replete nutrients or other dissolved compounds [27], [55], [66], while others deal with more generalized cases [58]. Certain models describe growth as a combination of various scaling factors derived from each input parameter [27], while others venture more deeply into the internal biological processes of the algae as it grows [55], [58], [66]. Many equations have been used to describe these scaling factors and biological processes [12], with constants and parameters

* Equal Contribution

Global Oceans 2020: Singapore - U.S. Gulf Coast | 978-1-7281-5446-6/20/$31.00 ©2020 IEEE | DOI: 10.1109/IEEECONF38699.2020.9389474

978-1-7281-5446-6/20/$31.00 ©2020 IEEE

taken either from existing relations and research [55], [66], or fitted to experimental data [22], [27], [49]. These models have largely delivered successful results for the conditions that they were designed for. However, selection of a model for alternate use requires it to be general and broad enough to include all parameters relevant to the given study in a meaningful way while not carrying too many irrelevant or unusable parameters.

The paper is organized as follows. In Sect. 2, we outline the methodology for exact optimal harvesting of algae fields in dynamic environments using autonomous tow vessels. The theory and schemes build upon the framework presented in [48] through state augmentation. We also present the numerical ocean modeling systems as well as the numerical model for the evolution of algae fields that we built upon the model by Ren et al. [58]. Sect. 3 demonstrates our methodology on several cases of increasing complexity. First, we consider the case of algae farms in fixed locations in space but under the influence of the dynamic ocean environment. This problem of visiting fixed farm locations using favorable dynamic currents and avoiding unfavorable ones can be solved with a method similar to that shown in [17]. Second, we consider the related case of an algae field that is spatially variable but anchored and not advected by currents. In our third case, the algae are no longer fixed in space. The dynamic ocean environment with strong currents can now advects the algae while biological mechanisms continue to influence its growth and decay. Our optimal harvesting then computes optimal collection paths for reactive algae fields that are advected by ocean currents. Finally, conclusions are presented in Sect. 4.

II. Methodology: Theory and Schemes

We now develop our formulation and outline numerical solvers for optimal harvesting path planning. Specifics of our ocean modeling systems that provide the dynamic fields inputs to the optimal harvesting are then presented. For the realistic simulations, we consider Nantucket Sound and Massachusetts Bay off the northeast US coast, and for the idealized simulations, a two-dimensional quasi-geostrophic double-gyre flow. Finally, we give an overview of our algae dynamic model.

A. Optimal Harvesting Path Planning

Our approach for collection-constrained path planning builds upon the traditional problem of time-optimal path planning. We first summarize the basic theory for exact time-optimal path planning [47], [48]. We then outline our augmentation of this theory to include field collection as a constraint to the optimization problem.

In traditional time-optimal path planning, a vehicle navigates in a domain $\mathbb{R}^d$ from a starting point $\boldsymbol{x}_s$ to a target $\boldsymbol{x}_f$ in fastest time. The vehicle moves at a speed F in an environment of dynamic flow field $\boldsymbol{V}(\boldsymbol{x},t)$. As outlined in [44], [48], the globally optimal solution to such path planning problem is governed by Hamilton-Jacobi equations for the reachability front and can be solved efficiently using the level set method. At a high level, this approach computes the optimal path by first propagating a reachability front (defined as the set of all states that can be reached by the vehicle at a given time) forward in time. This reachability front is represented as the zero level set of a function $\phi(\boldsymbol{x},t)$ and is a viscosity solution of an Hamilton-Jacobi equation. Following this forward solve, a backward trajectory solve is completed where the level sets of the computed function $\phi(\boldsymbol{x},t)$ are used to give the optimal headings of the vehicle and, in turn, the optimal path.

The forward solve for $\phi(\boldsymbol{x},t)$ is governed by the initial value Hamilton-Jacobi PDE given as follows

$$\begin{aligned}\frac{\partial\phi(\boldsymbol{x},t)}{\partial t}+F\left|\nabla\phi(\boldsymbol{x},t)\right|+\boldsymbol{V}(\boldsymbol{x},t)\cdot\nabla\phi(\boldsymbol{x},t)=0,\\ \phi(\boldsymbol{x},t=0)=\phi_0\end{aligned}\tag{1}$$

where the initial condition is a signed distance function from the start point: $\phi(\boldsymbol{x},t=0)=\phi_0=\|\boldsymbol{x}-\boldsymbol{x}_s\|$. The level-set Eq. (1) may be discretized and solved numerically. Furthermore, the PDE is solved until the time t_f such that $\phi(\boldsymbol{x}_f,t_f)=0$ (until the zero level set of $\phi(\boldsymbol{x},t)$ reaches the destination). Once the forward solve is completed, the optimal trajectory for the vehicle is obtained backward in time, by showing that at an arbitrary point in space and time, the optimal heading is normal to the level-set [48], i.e. it is given as $\boldsymbol{h}(t)=\frac{\nabla\phi(\boldsymbol{x},t)}{|\nabla\phi(\boldsymbol{x},t)|}$. The optimal trajectory, $\boldsymbol{x}_p(t)$, can be then shown to be governed by the ODE given as:

$$\begin{aligned}\frac{d\boldsymbol{x}_p(t)}{dt}&=-\boldsymbol{V}(\boldsymbol{x}_p,t)-F\frac{\nabla\phi(\boldsymbol{x}_p,t)}{|\nabla\phi(\boldsymbol{x}_p,t)|}\\ \boldsymbol{x}_p(t=t_f)&=\boldsymbol{x}_f.\end{aligned}\tag{2}$$

The backtracking equation (2) is solved backward in time starting from $\boldsymbol{x}=\boldsymbol{x}_f$ and $t=t_f$. For further details, we refer to [36], [44], [46]–[48].

The aforementioned theory governs time-optimal paths in dynamic flow fields. To now account for harvesting of an external field, these equations can be extended using state augmentation [6]. Consider a possibly dynamic field $\mathcal{H}(\boldsymbol{x},t)$ which must be harvested by the vehicle. Furthermore, if $\boldsymbol{x}_A=[\boldsymbol{x},c]^T$ is defined as an augmented state (where c is the amount of field collected by the vehicle and $\boldsymbol{x}$ is its position), the corresponding Hamilton-Jacobi level set equation for the function $\phi(\boldsymbol{x}_A,t)$ is given as:

$$\begin{aligned}\frac{\partial\phi(\boldsymbol{x}_A,t)}{\partial t}+F\left|\nabla\phi(\boldsymbol{x}_A,t)\right|+\boldsymbol{V}(\boldsymbol{x},t)\cdot\nabla_x\phi(\boldsymbol{x}_A,t)\\ +\mathcal{H}(\boldsymbol{x},t)\cdot\frac{\partial\phi}{\partial c}=0,\\ \phi(\boldsymbol{x}_A,t=0)=\phi_0\end{aligned}\tag{3}$$

where ∇_x is the gradient components in the physical domain. Moreover, the initial condition for the PDE is defined as $\phi(\boldsymbol{x}_A,t)=\phi_0=\left\|\boldsymbol{x}_A-[\boldsymbol{x}_s,c_s]^T\right\|$, where c_s is the initial amount of the harvesting field that the vehicle begins with at the start point. The backtracking equation is then given as:

$$\begin{aligned}\frac{d\boldsymbol{x}_p(t)}{dt}&=-\boldsymbol{V}(\boldsymbol{x}_p,t)-F\frac{\nabla_x\phi(\boldsymbol{x}_p,t)}{|\nabla_x\phi(\boldsymbol{x}_p,t)|}\\ \frac{dc_p(t)}{dt}&=-\mathcal{H}(\boldsymbol{x}_p,t)\\ \boldsymbol{x}_p(t=t_f)=\boldsymbol{x}_f,&\quad c_p(t=t_f)=c_f\end{aligned}\tag{4}$$

The corresponding path gives the time-optimal solution to the optimal collection problem. Specifically, if the vehicle starts at $\boldsymbol{x}_s$ with an initial amount c_s of the harvesting field, this path gives the quickest route such that the vehicle arrives at the target $\boldsymbol{x}_f$ with amount c_f of the field. In other words, it gives the path where the amount $c_f - c_s$ of the field is harvested from the environment as fast as possible.

An assumption made in the above equations is that the vehicle has a negligible influence on the field it is collecting. This must be assumed as the dynamics of the vehicle path cannot be incorporated into the external field during the solve. Therefore, the effect of the reduction in algae from the surrounding field cannot be imposed until the final path is computed. Fortunately, the length scales of the algal fields are typically orders of magnitude larger than the widths of the paths traced by the autonomous vessels, and so this assumption is then not too restrictive. Similarly, it is also common for the duration of the vehicle's mission to be limited (e.g. power constraints) such that the time required by the vehicle to complete its harvesting is typically short compared to the time-scales of the field to be harvested. In such cases, once a mission is completed, the harvested quantities can be removed from the field to be harvested at the right times along the vehicle path. The next path planning mission can then use this reduced field to be harvested.

B. Dynamic Ocean Environment Modeling

For this work, we utilized and developed our MIT-MSEAS modeling system [23], [25], [41], [50], including our hydrostatic PE code with a nonlinear free surface, based on second-order structured finite volumes, and a generalized biogeochemical model for lower trophic levels [40]. This MSEAS software is used for fundamental research and for realistic simulations and predictions in varied regions of the world's ocean [9], [18], [21], [26], [35], [39], [42], [45], [52], [56], [65], including monitoring [43], ecosystem prediction and environmental management [4], [10], and multi-disciplinary predictions and data assimilation [24], [38], [60]. Our modeling system can also simulate non-hydrostatic dynamics using a finite-volume framework [68] or finite-element codes [69].

Realistic Data-Assimilative Ocean Simulations. For the realistic simulations of Mass. Bay and Nantucket Sound off the northeast US coast that are inputs to the optimal harvesting, we employ our MSEAS-PE system.

The Mass. Bay set-up [24] has a 333 m horizontal resolution and 100 vertical levels with optimized level depths (e.g., in deeper water, higher resolution near the surface or large vertical derivatives, while at coasts, evenly spaced to minimize vertical CFL restrictions). The bathymetry was obtained from the 3 arc second USGS Gulf of Maine digital elevation model [67]. The sub-tidal initial and boundary conditions were downscaled from 1/12-degree Hybrid Coordinate Ocean Model (HYCOM) analyses [11], using our optimization for our higher resolution coastlines and bathymetry [23]. Local corrections were made using feature models and synoptic CTDs of opportunity. Tidal forcing was computed from the high resolution TPXO8-Atlas from OSU [14], [15], by reprocessing for our higher resolution bathymetry/coastline and quadratic bottom drag. The atmospheric forcing consisted of hourly analyses/forecasts of wind stresses, net heat flux, and surface freshwater flux from the 3 km North American Mesoscale Forecast System (NAM) [51].

The Nantucket Sound region set-up is similar, with the following differences. We employed implicit 2-way nested domains [25] with 600 m and 200 m horizontal resolutions and 20 terrain following levels in the vertical. In order to represent flow details not captured by the 1/12° HYCOM analyses, the subtidal initial and boundary conditions were created from a combination of objective analyses of synoptic data, SST and feature models for the coastal currents and the shelfbreak front.

Idealized Simulations. For idealized cases, we solve the 2D wind-driven barotropic single-layer model PDEs, the so-called double-gyre flow [48]. Our modular finite volume framework [68] is used to solve these PDEs as well as the PDE for the algae field dynamics, including advection-diffusion and a reaction term from our algae growth model, as discussed next.

C. Algae Dynamics Modeling

The algae growth model we use to simulate the fields for optimal collection is a modified version of the macroalgae growth model of Ren et al. [58]. The general applicability of this model and its inclusion of a wide array of environmental parameters and internal algae biological mechanisms allows us to explore different environmental growth conditions and simulation regimes. The Ren model provides algae concentrations as a function of the three state variables: Carbon, Nitrogen, and Phosphorous. Algae growth is linearly correlated to carbon growth, which can only occur under certain temperature, light, fluid flow, and internal state conditions, as modeled by:

$$U_C = G_{max} * C * f(T) * f(L) * f(Q_N) * f(Q_P) * f(V)\,. \quad (5)$$

In eq. (5), U_C is the carbon uptake rate, or scaled algae mass uptake rate; G_{max} the maximum carbon uptake rate; C the carbon concentration; and $f(T)$, $f(L)$, $f(Q_N)$, $f(Q_P)$, and $f(V)$ the effects on growth rate from temperature, light, Nitrogen quota, Phosphorous quota, and fluid velocity, respectively. The temperature and light functions $f(T)$ and $f(I)$ are defined respectively as an Arrhenius relationship comparing actual temperature to a set of biological references and a Lambert-Beer law to describe the behavior of light-attenuating materials in the water. The Nitrogen and Phosphorous quota functions $f(Q_N)$ and $f(Q_P)$ model the effect of internal nutrient ratios on the growth rate of the algae. The velocity function $f(V)$ is a Monond-type equation that models the dependence of algae growth on the flow field surrounding it. Formulations for these intermediate functions are in [58].

Nitrogen and phosphorous uptake rates, which dictate algae growth through $f(Q_N)$ and $f(Q_P)$ in eq. (5), are:

$$U_N = \frac{f(T) * C * (U_{NH} + U_{NO})}{1 + exp[(Q_N - Q_{Nmax})/Q_{Noff}]} \quad (6)$$

$$U_P = \frac{f(T) * C * U_{PO}}{1 + exp[(Q_P - Q_{Pmax})/Q_{Poff}]} \quad (7)$$

where U_N and U_P are the uptake rates of nitrogen and phosphorous, respectively; U_{NH}, U_{NO}, and U_{PO} the ammonium, nitrate, and phosphorus uptake rates defined by a type-II function response to concentrations in the surrounding water; and Q_N, Q_P, Q_{Nmax}, Q_{Pmax}, Q_{Noff}, and Q_{Poff} the nitrogen and phosphorous current quota values N/C and P/C, where N and P are the stored nitrogen and phosphorus values; nitrogen and phosphorus maximum quota values; and nitrogen and phosphorus storage switch transition width values, respectively.

These three uptake rate functions are used in a system of ODEs to calculate the algae growth over time:

$$\frac{dC}{dt} = U_C - \Phi_C \quad (8)$$

$$\frac{dN}{dt} = U_N - \Phi_N \quad (9)$$

$$\frac{dP}{dt} = U_P - \Phi_P \quad (10)$$

Here, $\Phi_{C,N,P}$ represent the death rate of each state variable:

$$\Phi_C = (k_r * f(T) + \omega_i + \omega_s) * C \quad (11)$$

$$\Phi_N = Q_N * \Phi_C - \epsilon_{up} * (U_{NO} + UNH) \quad (12)$$

$$\Phi_P = Q_P * \Phi_C - \epsilon_{up} * (U_P) \quad (13)$$

where k_r is the carbon respiration coefficient; ω_i the algae intrinsic morality (an exponential function of the difference between the environmental temperature and a trigger temperature for intrinsic morality); ω_s the oxygen stress morality (a Monond-type equation of the oxygen concentration below a threshold level); and ϵ_{up} the nutrient uptake associated excretion coefficient.

Environmental input fields to this point ODE system is taken from our MSEAS high resolution coupled physical-biogeochemical simulations (Sect. II-B). The fields called for in the system not available from these simulations include dissolved oxygen levels and environmental phosphorous availability. Both of these terms are assumed here to be uniformly replete throughout the domain. This assumption eliminates the dissolved oxygen growth death term ω_s in the carbon death rate term and sets U_{PO} to be uniformly equal to its maximum value U_{POmax}. Certain algae parameters are slightly modified to better fit algae growth to the northeast climates, such as the Arrhenius temperature constants used in $f(T)$. Detritus and zooplankton fields are used as particulate inorganic and particulate organic light-attenuating materials for the Lambert-Beer light function $f(I)$. For increased accuracy, the Ren model was also modified to use our instantaneous local flux of solar intensity accounting for cloud cover, as opposed to only seasonal fluctuations. Finally, a Monond-type scaling factor [5] modifies the carbon intrinsic morality term ω_i for more accurate results in our simulations.

III. Results

In this section, we illustrate our theory and schemes for algae dynamic modeling and optimal harvesting through three sets of examples. The first set (Sect. III-A) considers no algae dynamics and models the problem of having to time-optimally visit/monitor a set of farms (parametrized as points) in Nantucket Sound and return to the destination. In the second set (Sect. III-B), we introduce algae dynamics and consider the idealized case of collecting from kelp farms chained to the seafloor in Mass. Bay. In the final set (Sect. III-C), we consider dynamic algae fields that are advected by the external flow. This is also representative of cases where the goal is to collect harmful algae blooms or reactive pollutants. Two sub-cases are presented: (i) collection of algae in an idealized double-gyre flow and (ii) collection of fields biologically modeled in Mass. Bay. These cases are summarized in Table I.

Case Number	Case Description	Optimal Path Planning	Algae Dynamics	External Flow Algae Advection
1	Nantucket Sound Fixed Farms	x		
2	Mass. Bay Fixed Farm Fields	x	x	
3	Idealized Double Gyre Dynamics	x	x	x
	Mass. Bay Full Dynamic Fields	x	x	x

TABLE I: Summary of cases (crosses indicate what is active).

A. Case 1: Nantucket Sound – Multiple Farms Visits

In this application, we consider the problem of visiting, monitoring, or collecting from, distinct algae farms distributed in a dynamic ocean region. For each farm, some local operator (human or machine) could first amass the algae into a local stockpile. The task of the autonomous tow vessel is then to travel from a start to a target point while visiting farms along the way, e.g. to collect the assembled algae, all in fastest time. Due to the dynamic ocean currents, the autonomous vessel must optimally plan its path so as to reach the target in minimum time by using the currents to its advantage and by additionally selecting the order in which to visit the farms.

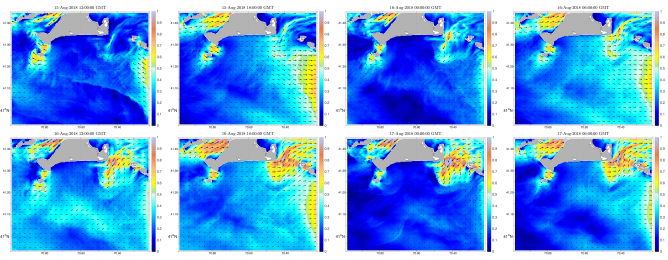

Fig. 1: Dynamic flow field in the Nantucket Sound region simulated using the MSEAS-PE model and plotted between 15 Aug. 2019 12Z and 16 Aug. 2019 06Z at 6 hour intervals.

We illustrate results for the case of algae farms distributed in Nantucket Sound (Fig. 1). The autonomous vessel, with a nominal speed of 1 m/sec, is tasked with leaving a harbour near the coast and visiting two farms before returning. This

scenario corresponds to multiple points-to-points time-optimal path planning in dynamic flows, of governing eqs. (1– 2). It is exactly solved by the algorithm outlined in [16]. Results for the time-optimal path are shown in Fig. 2, in which the harbour is shown as point A and the two algae farms as points B and C. Fig. 2a corresponds to the case of visiting first farm B and then farm C before returning to A, whereas Fig. 2b depicts the result for visiting farm C and then farm B before returning. Drawn additionally on each plot are the level sets of the function $\phi(\boldsymbol{x}, t)$. Three different forward solves are needed for each start-target combination, and a sample of the zero level set function are shown at a few times for each solve. The final optimal paths between the way-points are shown in red. The route ABCA takes 13 hours 54 min, saving 40 min compared to the route ACBA that takes 14 hours 34 min.

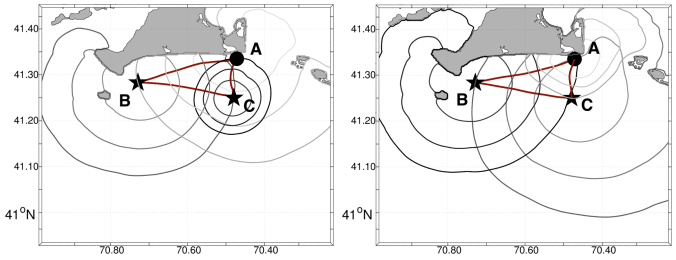

(a) A → B → C → A (b) A → C → B → A

Fig. 2: The time optimal paths (red) to travel from the start point (A) to the algae farms (B and C) and back. (a) The optimal route to go from A to B to C and return. (b) The optimal route to go from A to C to B and return. The route in (a) saves 40 minutes compared to the route in (b).

In presence of a higher number of farms, the number of possible routes is $n!$. An optimal way to cheaply check all of these routes by reusing certain legs between two points and by parallelizing various computations is discussed in [17].

B. Case 2: Mass. Bay – Harvesting of Kelp Farm Fields

Unlike many other forms of algae that float freely in water, kelp are anchored to the seafloor by holdfasts and do not advect with ocean currents. Recent work with Saccharina latissima, or sugar kelp, has seen the development of novel cultivation [31] and new investigation into kelp use not only as a traditional crop but also as a waste nutrient extractor and a vehicle for carbon sequestration [33]. Recently, farming applications with sugar kelp have also been carried out in Southern New England [71].

While kelp are anchored to the sea floor, their growth is affected by dynamic spatially dependent environmental variables such as temperature, light, and nutrients. In our case, we simulate the spatially dependent growth of a stationary kelp farm field in Mass. Bay. The dynamic inputs involve: i) nitrate, ammonium, chlorophyll, zooplankton and detritus fields from our high-resolution coupled physical-biogeochemical simulations (Sect. II-B), and ii) our modified algae growth model (Sect. II-C). We then apply our augmented path planning theory and schemes (Sect. II-A) to optimally plan for harvesting from these farm fields.

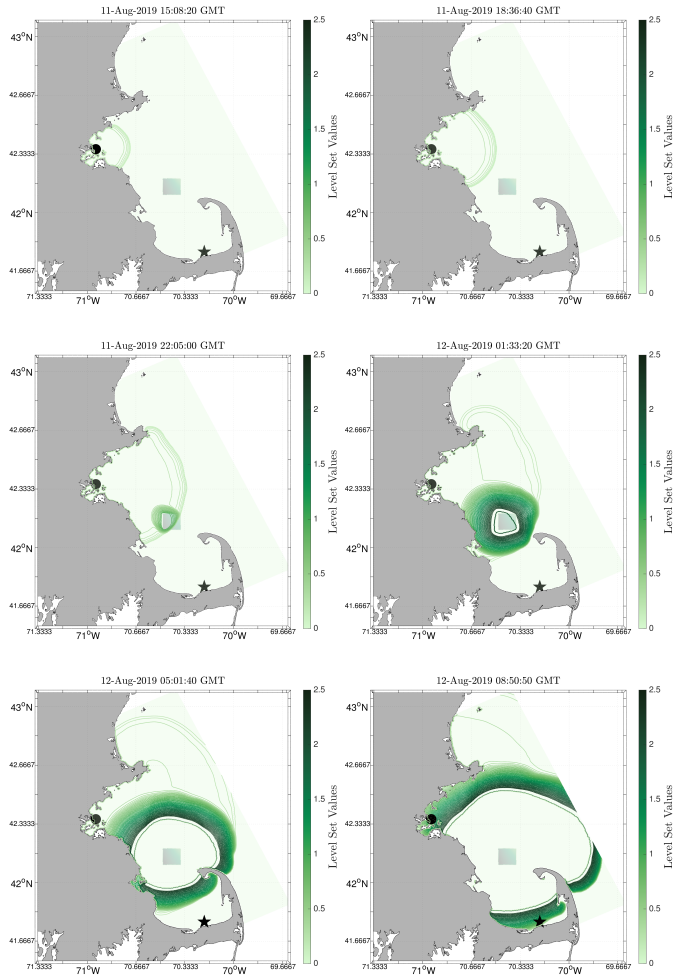

Fig. 3: Start point (Boston Harbor at 11 Aug 2019 12 Z - full circle) and end point (Dennis, Cape Cod - star, optimally reached at 12 Aug 2019 08:51 Z) of the vehicle and evolution of the augmented forward level set. The 2D level-set contours pictured represent the 3D reachability front at various collection levels. The colorbar represents how much algae is collected for each of the reachability contour, i.e. the color of a reachability contour corresponds to the maximum amount of algae a vehicle inside that front could have collected.

Fig. 3 illustrates the forward results, the dynamic evolution of the augmented forward reachability front. The autonomous vehicle starts in Boston Harbor at 12Z, 11 Aug. 2019, with a desired end point near Dennis. The rectangle just off Stellwagen Bank is the farm field. The field has been colored based on the kelp collection rate (in units of [units of kelp] / [time]) – high values correspond to regions in the farm where the kelp concentration is higher which results in the corresponding higher collection rate. Overlaid on the different panels are 2D contours of the 3D reachability front at the times shown. Recall that this reachability front is indeed in a 3D augmented space – the 2D physical space with an additional dimension for the collected algae/kelp amount. The color of the contour represents the maximum amount of kelp that a vehicle could have collected by that time at that location of the front. The

reachability front approaches the kelp farm with the contour values unchanged (see the 15:08 Z and 18:36 Z snapshots). This is because no algae field was encountered and so no collection was performed. At 22:05 GMT, the front reaches the kelp farm, resulting in the contour values increasing, indicative of algae being collected. Having increased in the kelp farm region, the front then expands until the destination. Fig. 4 shows the final optimal path as obtained by solving eq. (4). The vehicle reaches the end point with the desired kelp amount of 1.5 units at 8:51 Z on the next day (12 Aug 2019).

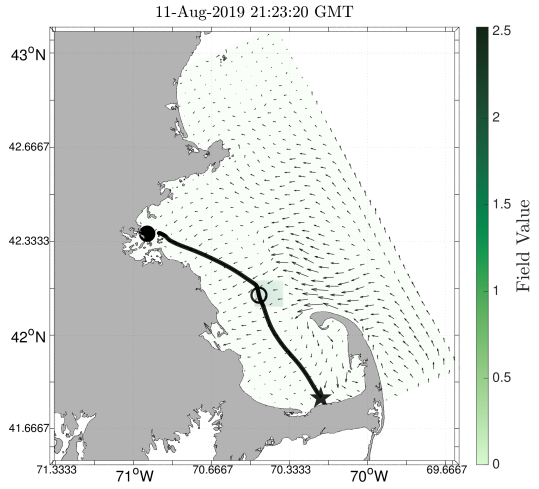

Fig. 4: The globally-optimal path from start (full circle) to finish (star) while collecting the required amount of algae from the boxed farm region. A snapshot is shown at an intermediate time on the way to the destination via the farm (circle). Shown in the background is the kelp collection rate field (in units of $\frac{\text{[units of kelp]}}{\text{[time]}}$) – high values correspond to regions in the farm where the kelp concentration is higher, which results in the higher collection rate.

C. Case 3: Dynamic Algae Fields with Flow Advection

An example of dynamic algae fields are harmful algae blooms (HABs) that occur due to a range of reasons including rising temperatures and nutrient-rich wastewater runoff [61], leading to large colonies of micro or macro algae growing at rapid rates. HABs have been observed in all 50 states in the U.S., in large freshwater lakes, small inland lakes, rivers, reservoirs, and marine coastal areas and estuaries. These HABs can create low-oxygen dead zones [20], [28], release toxins that are harmful to humans and animals, displace indigenous species, alter habitats and ecosystems [1], and lead to millions of dollars of economic losses each year through public health effects, commercial fishery impacts, medical expenses, and lost work days [64]. Our optimal path planning proposed here can help both monitor and control HABs.

The dynamics of HAB growth is not fully understood. To enhance incomplete models, common forecasts utilize satellite and in-situ data [64]. Traditional in-situ sampling methods are reactive, slow to respond, and operate with fixed time and spatial sampling grids, leading to calls to use AUVs for improved data collection [13], [59], [62]. These AUVs would greatly benefit from our optimal theory.

In addition to modeling and monitoring, many control strategies for HABs have been proposed. These include flocculation, sediment resuspension, burial, harvesting, water column mixing, biological control, and genetic engineering as well as the targeted release of allelochemicals, biosurfactants, hydrogen peroxide, copper sulfate, and silica [1], [32], [53]. Once areas where HABs are likely or have begun growing are known, our optimal path planning would deliver control strategies in an efficient and cost-effective manner to at-risk areas and so reduce ecological and economic damage.

In the following results, we showcase our optimal harvesting as a control strategy to tackle HABs, using autonomous vehicles to collect such dynamic algae fields time-optimally. In all cases, the algae growth and decay is modeled along with its advection due to the environmental flow field.

1) Double-Gyre Flow Advecting a Dynamic Algae Field: In this first sub-case, we consider optimal algae collection in an idealized double-gyre flow field (Fig. 5). This flow simulates near-surface ocean circulation at mid-latitude regions, where easterlies and trade winds in the northern hemisphere drive a cyclonic and an anticyclonic gyre with the zonal jet in between (e.g. an idealized version of the Gulf Stream) [48].

The fluid flow is governed by the non-dimensional PDEs:

$$\begin{aligned}\frac{\partial u}{\partial t} &= \frac{\partial p}{\partial x} + \frac{1}{\text{Re}}\Delta u - \frac{\partial (u^2)}{\partial x} - \frac{\partial (uv)}{\partial y} + fv + a\tau_x \\ \frac{\partial v}{\partial t} &= \frac{\partial p}{\partial y} + \frac{1}{\text{Re}}\Delta v - \frac{\partial (uv)}{\partial x} - \frac{\partial (v^2)}{\partial y} - fu + a\tau_y \\ 0 &= \frac{\partial u}{\partial x} + \frac{\partial v}{\partial y} \end{aligned} \tag{14}$$

which are solved numerically (Sect. II-B). For the case shown, a flow Reynolds number of 150 was used with $f = \tilde{f} + \beta y$, the non-dimensional Coriolis coefficient, and $a = 10^3$, the strength of the wind stress. In non-dimensional terms, we use $\tilde{f} = 0, \beta = 10^3$. The flow in the basin is forced by an idealized steady zonal wind stress, $\tau_x = -\frac{1}{2\pi} cos\ 2\pi y$ and $\tau_y = 0$.

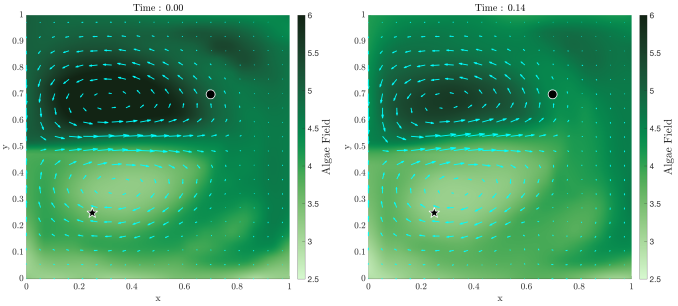

Fig. 5: Snapshots of the environment at non-dimensional times 0 and 0.14 with the unsteady velocity fields overlaid on an algae collection rate field (in units of $\frac{\text{[units of algae]}}{\text{[time]}}$) – high values correspond to regions where the algae concentration is higher resulting in a higher collection rate. Start (full circle) and end (star) points of the vehicle are shown.

We employ our modified algae growth model (Sect. II-C). All relevant environmental parameters are assumed constant

except for the three nutrient fields (nitrate, ammonium, phosphorus) and the light field. The spatially varying light field is lower intensity toward the left hand side of the domain ($x < 0.5$) and higher intensity toward the right hand side of the domain ($x > 0.5$) to simulate cloud coverage impairing the growth of the initial high-concentration area (see upper left of the two snapshots in Fig. 5). In addition, the initial values for the three nutrient fields are assigned high and low concentration areas throughout the domain to simulate spatial variability in the algae growth rate. To solve the advection-diffusion-reaction algae field dynamics, we use a QUICK scheme in our finite-volume framework (Sect. II-B).

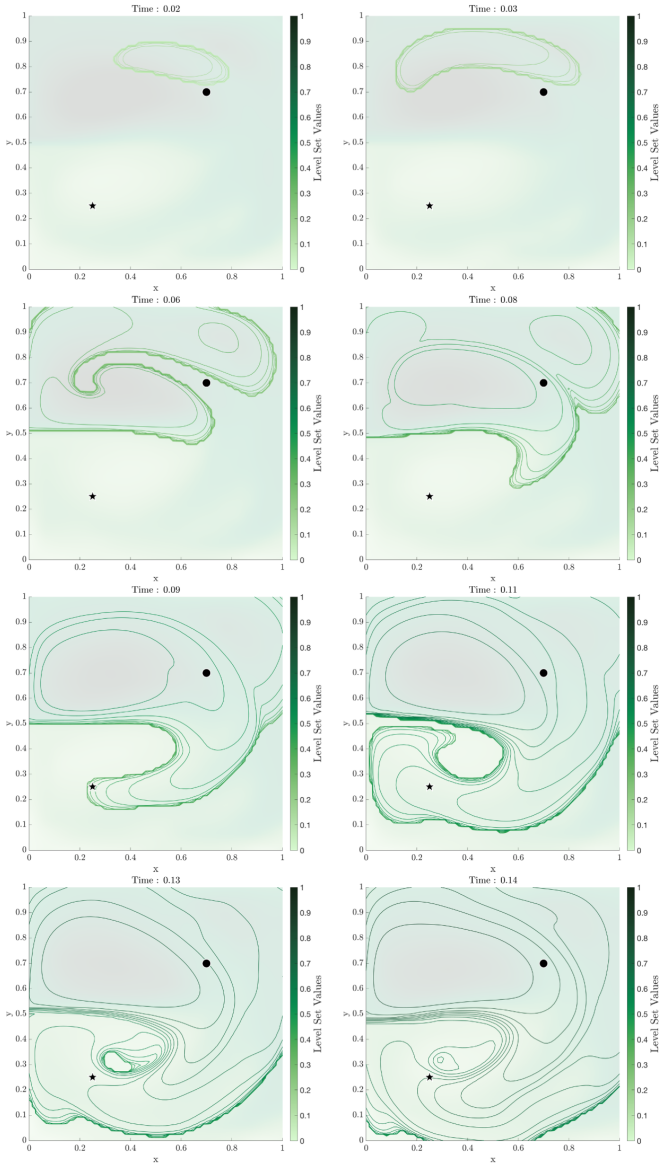

Fig. 6: Snapshots of the level set at various points in time. Since the level set is a surface in an augmented space (2D physical space and an additional dimension for the collected algae amount), the constant algae collection amount contours of this surface are shown. The level set evolves until it attains a value of 0.7 units at the target.

In this sub-case, we demonstrate an optimal collection with the constraint of having to collect at least 0.7 units of algae before reaching the destination. Fig. 5 shows the dynamic environment at two times, with two gyres, the jet, and the algae field dynamically evolving and transported by the flow.

Fig. 6 shows the evolution of the 3D reachability front. As required, these 2D contours (slices of the 3D front) evolve until the level set value of 0.7 units is reached at the target.

The final computed optimal path is in Fig. 7. The path clearly evolves to remain in the areas of high concentration, while simultaneously using the external currents to its advantage and reach the target as fast as possible. It is important to reiterate that this computed path is *globally optimal*; no other path from the start to the end point exists in which the vehicle can reach faster while collecting 0.7 units of the field.

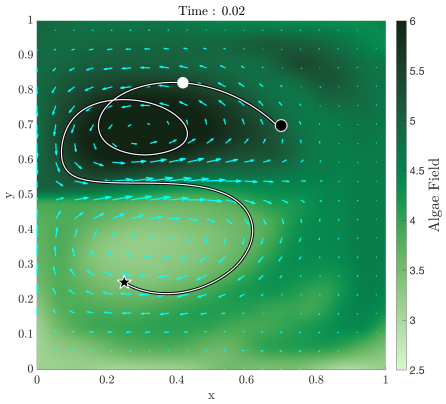

Fig. 7: The final computed globally-optimal path for the algae collection problem with the vehicle (white circle) shown traversing it at some intermediate time.

2) Mass. Bay – Harvesting Dynamic Chlorophyll Fields: For the second sub-case, we consider the Mass. Bay region. We showcase an alternate control strategy to monitor harmful algal blooms: the study of chlorophyll fields. Various studies have shown that the concentration of chlorophyll (particularly chlorophyll-a) provides a direct measurement of algae growth in aquatic environments [30]. This close connection between chlorophyll and algae has been exploited in several research avenues for predicting harmful algal blooms [2], [62], [64] and here motivates our collection of dynamic chlorophyll fields.

Our high-resolution coupled physical-biogeochemical simulations (Sect. II-B) are used to model the ocean currents (Fig. 8) as well as the chlorophyll field.

Using our theory and schemes for optimal harvesting (Sect. II-A), we plan the path of a vehicle that travels from a start point to a destination while optimally collecting chlorophyll along the way. Fig. 9 shows the evolution of the level sets from the forward solve. Here, as before, the reachability front evolves at almost a constant collected algae value until it reaches offshore from Scituate. In this region, chlorophyll has bloomed which results in a corresponding increase in the reachability front value (at 3:40 GMT for instance). The front then, as before, expands until it reaches the target point with the desired final algae field amount of 0.4 units.

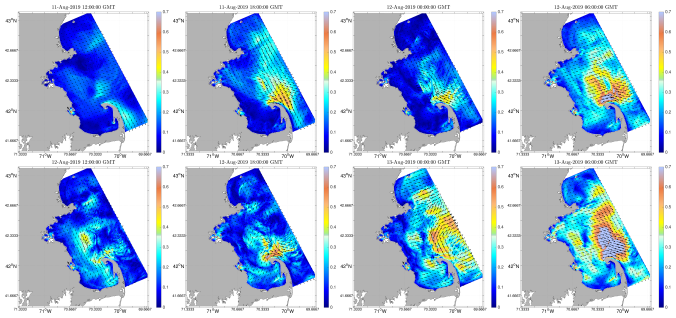

Fig. 8: Dynamic velocity field in Mass. Bay simulated using our data-assimilative MSEAS-PE modeling system and plotted between 11 and 13 Aug. 2019.

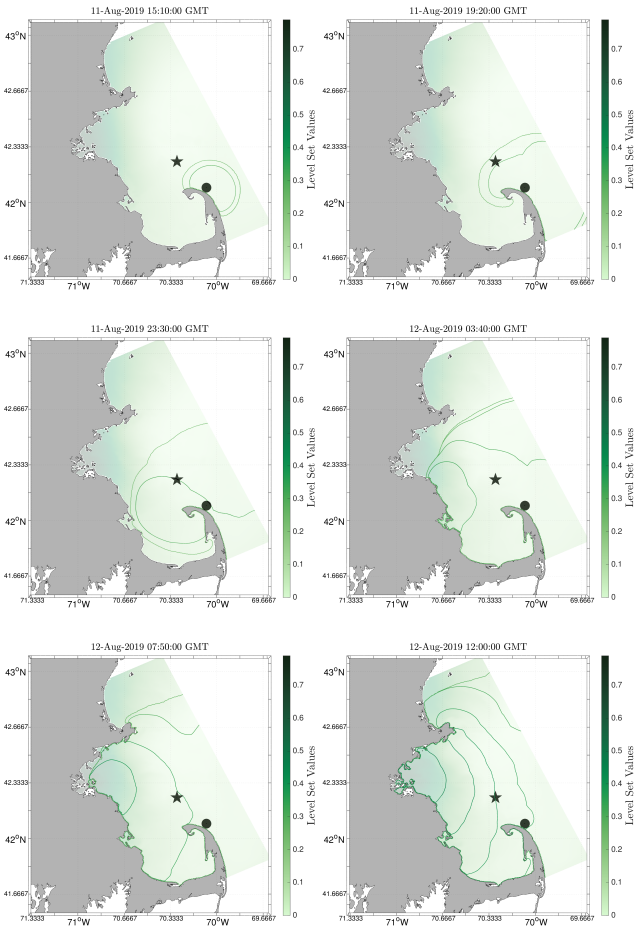

Fig. 9: Evolution of the forward level set. The background represents the concentration of Chlorophyll from our MSEAS PE-bio simulation at that time. The contours shown represent the reachability front at various collection levels.

Fig. 10 shows the final optimal path computed using eq. (4). As expected, the autonomous vessel's optimal path takes it to high algae concentration regions offshore from Scituate to harvest just enough of the field before starting its return journey to the target. The vehicle reaches the end point with the desired algae amount of 0.4 units at 12 Z 12 Aug 2019.

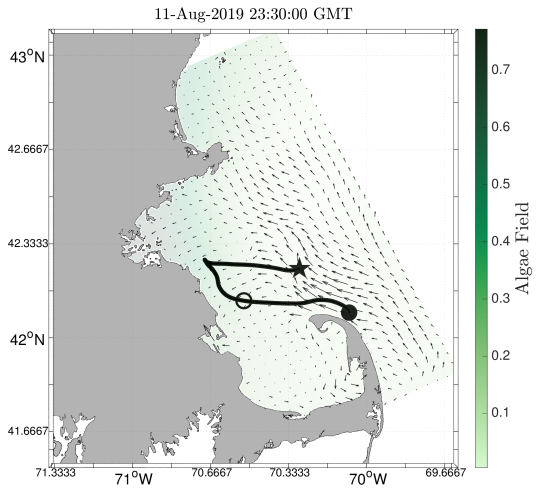

Fig. 10: The final globally-optimal path from start (full circle) to finish (star) while collecting the required amount of Chlorophyll. A snapshot is shown at an intermediate time (vehicle shown as the circle). Shown in the background is the spatially varying Chlorophyll collection rate field (in units of $\frac{[\text{units of Chl}]}{[\text{time}]}$) – high values correspond to regions where the concentration of Chlorophyll is higher resulting in a higher collection rate.

IV. Conclusion

In this work, we addressed two challenges to the efficient operation of offshore algae farming: (i) accurate models of the dynamic ocean environment including macroalgae ecosystem dynamics and (ii) intelligent path planning algorithms for autonomous vessels that optimally manage and harvest the algae fields. We first integrated our numerical modeling system of the ocean environment with a numerical model for forecasting the growth and decay of algae fields. These fields are then input into our exact optimal path planning, augmented with the optimal harvesting goals and solved using level set methods. The resulting path is a provable time-optimal route for the vehicle to follow under the constraint of having to monitor or harvest a specified amount of the field to collect. We demonstrated our theory with simulated algal growth in both idealized and realistic data-assimilative dynamic ocean environments and computed the optimal paths for an autonomous collection vehicle.

We showed that our theory and schemes can be used to compute accurate optimal path in a variety of scenarios. Our first case considered the problem of time-optimal path planning between point farms at fixed spatial locations, where the vehicle was required to visit each farm while navigating optimally in the dynamic ocean environment. We then relaxed the point farm assumption and considered the case of spatially varying algae farm fields fixed in space (e.g. kelp farms). For this, an algae dynamic model predicted the growth and decay of the algae field, which was then used to inform the optimal paths to harvest. Finally, our third case added the complexity of collecting algae fields no longer fixed in space but also

advected by currents. An example of this case is the optimal harvesting of harmful algal blooms. We first demonstrated the optimal harvesting for an idealized double gyre flow scenario and our dynamic algae model with advection. Finally, we showcased the scenario of optimal harvesting a dynamic Chlorophyll field in realistic data-assimilative simulations of the physical-biogeochemical Mass. Bay environment. All these results are very promising for a wide range of future optimal ocean monitoring and harvesting.

ACKNOWLEDGMENT

We thank all members of the MSEAS group, past and present. In particular, we thank Abhinav Gupta for his input regarding the implementation of the algae dynamic models used in this work. We are grateful to the DOE - Office of ARPA-E for support under grant DE-AR0000910 (MARINER) to MIT. We thank the HYCOM team for their ocean fields, NMFS (Tamara Holzwarth-Davis and Paula Fratantoni) for their survey CTD data, NCEP (Matthew Pyle, Eric Rogers, Geoff DiMego, and Arun Chawla) for their help and support for atmospheric forcing forecasts, NOAA NDBC for supplying buoy data, JHU APL for processed SST images, and CORDC for HF Radar data.

REFERENCES

[1] D. M. Anderson. Approaches to monitoring, control and management of harmful algal blooms (HABs). *Ocean & coastal management*, 52(7):342, July 2009.

[2] S. M. J. Baban. Trophic classification and ecosystem checking of lakes using remotely sensed information. *Hydrological Sciences Journal*, 41(6):939–957, Dec. 1996.

[3] J. Barraquand, B. Langlois, and J.-C. Latombe. Numerical potential field techniques for robot path planning. *IEEE transactions on systems, man, and cybernetics*, 22(2):224–241, 1992.

[4] Ş. T. Beşiktepe, P. F. J. Lermusiaux, and A. R. Robinson. Coupled physical and biogeochemical data-driven simulations of Massachusetts Bay in late summer: Real-time and post-cruise data assimilation. *Journal of Marine Systems*, 40–41:171–212, 2003.

[5] G. Bendoricchio, G. Coffaro, and C. De Marchi. A trophic model for Ulva rigida in the Lagoon of Venice. *Ecological Modelling*, 75-76:485–496, Sept. 1994.

[6] M. Bhabra, M. Doshi, and P. F. J. Lermusiaux. Harvesting constrained time optimal path planning. *In preparation*, 2020.

[7] C. A. Goudey and Associates. C. A. Goudey and Associates (http://cagoudey.com), June 2020.

[8] K. P. Carroll, S. R. McClaran, E. L. Nelson, D. M. Barnett, D. K. Friesen, and G. N. William. Auv path planning: an a* approach to path planning with consideration of variable vehicle speeds and multiple, overlapping, time-dependent exclusion zones. In *Proceedings of the 1992 Symposium on Autonomous Underwater Vehicle Technology*, pages 79–84. IEEE, 1992.

[9] M. E. G. D. Colin, T. F. Duda, L. A. te Raa, T. van Zon, P. J. Haley, Jr., P. F. J. Lermusiaux, W. G. Leslie, C. Mirabito, F. P. A. Lam, A. E. Newhall, Y.-T. Lin, and J. F. Lynch. Time-evolving acoustic propagation modeling in a complex ocean environment. In *OCEANS - Bergen, 2013 MTS/IEEE*, pages 1–9, 2013.

[10] G. Cossarini, P. F. J. Lermusiaux, and C. Solidoro. Lagoon of Venice ecosystem: Seasonal dynamics and environmental guidance with uncertainty analyses and error subspace data assimilation. *Journal of Geophysical Research: Oceans*, 114(C6), June 2009.

[11] J. A. Cummings and O. M. Smedstad. *Variational Data Assimilation for the Global Ocean*, pages 303–343. Springer Berlin Heidelberg, Berlin, Heidelberg, 2013.

[12] P. Darvehei, P. A. Bahri, and N. R. Moheimani. Model development for the growth of microalgae: A review. *Renewable and Sustainable Energy Reviews*, 97:233–258, Dec. 2018.

[13] C. Denniston, A. Kumaraguru, and G. S. Sukhatme. Comparison of Path Planning Approaches for Harmful Algal Bloom Monitoring. In *OCEANS 2019 MTS/IEEE SEATTLE*, pages 1–9, Oct. 2019. ISSN: 0197-7385.

[14] G. D. Egbert and S. Y. Erofeeva. Efficient inverse modeling of barotropic ocean tides. *Journal of Atmospheric and Oceanic Technology*, 19(2):183–204, 2002.

[15] G. D. Egbert and S. Y. Erofeeva. OSU tidal inversion, 2013.

[16] D. Ferris. Time-optimal multi-waypoint mission planning in dynamic flow fields. Master's thesis, Massachusetts Institute of Technology, Department of Mechanical Engineering, Cambridge, Massachusetts, June 2018.

[17] D. L. Ferris, D. N. Subramani, C. S. Kulkarni, P. J. Haley, and P. F. J. Lermusiaux. Time-optimal multi-waypoint mission planning in dynamic environments. In *OCEANS Conference 2018*, Charleston, SC, Oct. 2018. IEEE.

[18] A. Gangopadhyay, P. F. Lermusiaux, L. Rosenfeld, A. R. Robinson, L. Calado, H. S. Kim, W. G. Leslie, and P. J. Haley, Jr. The California Current system: A multiscale overview and the development of a feature-oriented regional modeling system (FORMS). *Dynamics of Atmospheres and Oceans*, 52(1–2):131–169, Sept. 2011. Special issue of Dynamics of Atmospheres and Oceans in honor of Prof. A. R. Robinson.

[19] B. Garau, A. Alvarez, and G. Oliver. Path planning of autonomous underwater vehicles in current fields with complex spatial variability: an a* approach. In *Proceedings of the 2005 IEEE international conference on robotics and automation*, pages 194–198. IEEE, 2005.

[20] A. W. Griffith and C. J. Gobler. Harmful algal blooms: A climate change co-stressor in marine and freshwater ecosystems. *Harmful Algae*, 91:101590, Jan. 2020.

[21] A. Gupta, P. J. Haley, D. N. Subramani, and P. F. J. Lermusiaux. Fish modeling and Bayesian learning for the Lakshadweep Islands. In *OCEANS 2019 MTS/IEEE SEATTLE*, pages 1–10, Seattle, Oct. 2019. IEEE.

[22] H. Haario, L. Kalachev, and M. Laine. Reduced Models of Algae Growth. *Bulletin of mathematical biology*, 71:1626–48, June 2009.

[23] P. J. Haley, Jr., A. Agarwal, and P. F. J. Lermusiaux. Optimizing velocities and transports for complex coastal regions and archipelagos. *Ocean Modeling*, 89:1–28, 2015.

[24] P. J. Haley, Jr., A. Gupta, C. Mirabito, and P. F. J. Lermusiaux. Towards Bayesian ocean physical-biogeochemical-acidification prediction and learning systems for Massachusetts Bay. In *OCEANS 2020 IEEE/MTS*. IEEE, Oct. 2020. In press.

[25] P. J. Haley, Jr. and P. F. J. Lermusiaux. Multiscale two-way embedding schemes for free-surface primitive equations in the "Multidisciplinary Simulation, Estimation and Assimilation System". *Ocean Dynamics*, 60(6):1497–1537, Dec. 2010.

[26] P. J. Haley, Jr., P. F. J. Lermusiaux, A. R. Robinson, W. G. Leslie, O. Logoutov, G. Cossarini, X. S. Liang, P. Moreno, S. R. Ramp, J. D. Doyle, J. Bellingham, F. Chavez, and S. Johnston. Forecasting and reanalysis in the Monterey Bay/California Current region for the Autonomous Ocean Sampling Network-II experiment. *Deep Sea Research Part II: Topical Studies in Oceanography*, 56(3–5):127–148, Feb. 2009.

[27] S. K. Jayaraman and R. R. Rhinehart. Modeling and Optimization of Algae Growth. *Industrial & Engineering Chemistry Research*, 54(33):8063–8071, Aug. 2015. Publisher: American Chemical Society.

[28] Joyce S. The dead zones: oxygen-starved coastal waters. *Environmental Health Perspectives*, 108(3):A120–A125, Mar. 2000. Publisher: Environmental Health Perspectives.

[29] T. Juracsek. Algae farming. Technical report, Overview 4/25, 2013.

[30] S. Karki, M. Sultan, R. Elkadiri, and T. Elbayoumi. Mapping and forecasting onsets of harmful algal blooms using modis data over coastal waters surrounding charlotte county, florida. *Remote Sensing*, 10(10):1656, 2018.

[31] P. D. Kerrison, M. S. Stanley, and A. D. Hughes. Textile substrate seeding of Saccharina latissima sporophytes using a binder: An effective method for the aquaculture of kelp. *Algal Research*, 33:352–357, July 2018.

[32] D. Kidwell. Programmatic Environmental Assessment for the Prevention, Control, and Mitigation of Harmful Algal Blooms Program. Technical report, National Oceanic and Atmospheric Administration, Feb. 2015.

[33] J. K. Kim, G. P. Kraemer, and C. Yarish. Use of sugar kelp aquaculture in Long Island Sound and the Bronx River Estuary for nutrient extraction. *Marine Ecology Progress Series*, 531:155–166, July 2015.

[34] J. J. Kuffner and S. M. LaValle. Rrt-connect: An efficient approach to single-query path planning. In *Proceedings 2000 ICRA. Millennium Conference. IEEE International Conference on Robotics and Automation. Symposia Proceedings (Cat. No. 00CH37065)*, volume 2, pages 995–1001. IEEE, 2000.

[35] C. S. Kulkarni, P. J. Haley, Jr., P. F. J. Lermusiaux, A. Dutt, A. Gupta, C. Mirabito, D. N. Subramani, S. Jana, W. H. Ali, T. Peacock, C. M. Royo, A. Rzeznik, and R. Supekar. Real-time sediment plume modeling in the Southern California Bight. In *OCEANS Conference 2018*, Charleston, SC, Oct. 2018. IEEE.

[36] C. S. Kulkarni and P. F. J. Lermusiaux. Three-dimensional time-optimal path planning in the ocean. *Ocean Modelling*, 152, Aug. 2020.

[37] S. M. Lavalle. Rapidly-exploring random trees: A new tool for path planning. TR 98-11, Iowa State University, Ames, IA, 1998.

[38] P. F. J. Lermusiaux. On the mapping of multivariate geophysical fields: Sensitivities to size, scales, and dynamics. *Journal of Atmospheric and Oceanic Technology*, 19(10):1602–1637, 2002.

[39] P. F. J. Lermusiaux, M. Doshi, C. S. Kulkarni, A. Gupta, P. J. Haley, Jr., C. Mirabito, F. Trotta, S. J. Levang, G. R. Flierl, J. Marshall, T. Peacock, and C. Noble. Plastic pollution in the coastal oceans: Characterization and modeling. In *OCEANS 2019 MTS/IEEE SEATTLE*, pages 1–10, Seattle, Oct. 2019. IEEE.

[40] P. F. J. Lermusiaux, C. Evangelinos, R. Tian, P. J. Haley, Jr, J. J. McCarthy, N. M. Patrikalakis, A. R. Robinson, and H. Schmidt. Adaptive coupled physical and biogeochemical ocean predictions: A conceptual basis. In *Computational Science - ICCS 2004*, volume 3038 of *Lecture Notes in Computer Science*, pages 685–692. Springer Berlin Heidelberg, 2004.

[41] P. F. J. Lermusiaux, P. J. Haley, W. G. Leslie, A. Agarwal, O. Logutov, and L. J. Burton. Multiscale physical and biological dynamics in the Philippine Archipelago: Predictions and processes. *Oceanography*, 24(1):70–89, 2011. Special Issue on the Philippine Straits Dynamics Experiment.

[42] P. F. J. Lermusiaux, P. J. Haley, Jr., S. Jana, A. Gupta, C. S. Kulkarni, C. Mirabito, W. H. Ali, D. N. Subramani, A. Dutt, J. Lin, A. Shcherbina, C. Lee, and A. Gangopadhyay. Optimal planning and sampling predictions for autonomous and Lagrangian platforms and sensors in the northern Arabian Sea. *Oceanography*, 30(2):172–185, June 2017. Special issue on Autonomous and Lagrangian Platforms and Sensors (ALPS).

[43] P. F. J. Lermusiaux, P. J. Haley, Jr, and N. K. Yilmaz. Environmental prediction, path planning and adaptive sampling: sensing and modeling for efficient ocean monitoring, management and pollution control. *Sea Technology*, 48(9):35–38, 2007.

[44] P. F. J. Lermusiaux, D. N. Subramani, J. Lin, C. S. Kulkarni, A. Gupta, A. Dutt, T. Lolla, P. J. Haley, Jr., W. H. Ali, C. Mirabito, and S. Jana. A future for intelligent autonomous ocean observing systems. *Journal of Marine Research*, 75(6):765–813, Nov. 2017. The Sea. Volume 17, The Science of Ocean Prediction, Part 2.

[45] W. G. Leslie, A. R. Robinson, P. J. Haley, Jr, O. Logutov, P. A. Moreno, P. F. J. Lermusiaux, and E. Coelho. Verification and training of real-time forecasting of multi-scale ocean dynamics for maritime rapid environmental assessment. *Journal of Marine Systems*, 69(1):3–16, 2008.

[46] S. V. T. Lolla. *Path Planning and Adaptive Sampling in the Coastal Ocean*. PhD thesis, Massachusetts Institute of Technology, Department of Mechanical Engineering, Cambridge, Massachusetts, Feb. 2016.

[47] T. Lolla, P. J. Haley, Jr., and P. F. J. Lermusiaux. Time-optimal path planning in dynamic flows using level set equations: Realistic applications. *Ocean Dynamics*, 64(10):1399–1417, 2014.

[48] T. Lolla, P. F. J. Lermusiaux, M. P. Ueckermann, and P. J. Haley, Jr. Time-optimal path planning in dynamic flows using level set equations: Theory and schemes. *Ocean Dynamics*, 64(10):1373–1397, 2014.

[49] A. Mazzelli, A. Cicci, F. Di Caprio, P. Altimari, L. Toro, G. Iaquaniello, and F. Pagnanelli. Multivariate modeling for microalgae growth in outdoor photobioreactors. *Algal Research*, 45:101663, Jan. 2020.

[50] MSEAS Group. MSEAS Software, 2013.

[51] National Centers for Environmental Prediction (NCEP). North American Mesoscale Forecast System (NAM). https://www.emc.ncep.noaa.gov/index.php?branch=NAM, Sept. 2019.

[52] R. Onken, A. Álvarez, V. Fernández, G. Vizoso, G. Basterretxea, J. Tintoré, P. Haley, Jr., and E. Nacini. A forecast experiment in the Balearic Sea. *Journal of Marine Systems*, 71(1-2):79–98, 2008.

[53] M. Pal, P. J. Yesankar, A. Dwivedi, and A. Qureshi. Biotic control of harmful algal blooms (HABs): A brief review. *Journal of Environmental Management*, 268:110687, Aug. 2020.

[54] T. V. R. Pillay, M. N. Kutty, et al. *Aquaculture: principles and practices*. Blackwell publishing, Oxford, UK, 2 edition, 2005.

[55] J. Quinn, L. de Winter, and T. Bradley. Microalgae bulk growth model with application to industrial scale systems. *Bioresource Technology*, 102(8):5083–5092, Apr. 2011.

[56] S. R. Ramp, P. F. J. Lermusiaux, I. Shulman, Y. Chao, R. E. Wolf, and F. L. Bahr. Oceanographic and atmospheric conditions on the continental shelf north of the Monterey Bay during August 2006. *Dynamics of Atmospheres and Oceans*, 52(1–2):192–223, Sept. 2011. Special issue of Dynamics of Atmospheres and Oceans in honor of Prof. A. R. Robinson.

[57] D. Rao and S. B. Williams. Large-scale path planning for underwater gliders in ocean currents. In *Australasian conference on robotics and automation (ACRA)*, pages 2–4, 2009.

[58] J. Ren, N. Barr, K. Scheuer, D. Schiel, and J. Zeldis. A dynamic growth model of macroalgae: Application in an estuary recovering from treated wastewater and earthquake-driven eutrophication. *Estuarine, Coastal and Shelf Science*, 148, July 2014.

[59] I. C. Robbins, G. J. Kirkpatrick, S. M. Blackwell, J. Hillier, C. A. Knight, and M. A. Moline. Improved monitoring of HABs using autonomous underwater vehicles (AUV). *Harmful Algae*, 5(6):749–761, Dec. 2006.

[60] A. R. Robinson and P. F. J. Lermusiaux. Prediction systems with data assimilation for coupled ocean science and ocean acoustics. In A. Tolstoy et al, editor, *Proceedings of the Sixth International Conference on Theoretical and Computational Acoustics*, pages 325–342. World Scientific Publishing, 2004. Refereed invited Keynote Manuscript.

[61] D. G. I. Schmale, A. P. Ault, W. Saad, D. T. Scott, and J. A. Westrick. Perspectives on Harmful Algal Blooms (HABs) and the Cyberbiosecurity of Freshwater Systems. *Frontiers in Bioengineering and Biotechnology*, 7, 2019. Publisher: Frontiers.

[62] O. Schofield, J. Bosch, S. Glenn, G. Kirkpatrick, J. Kerfoot, S. Lohrenz, M. A. Moline, M. Oliver, and P. Bissett. Bio-optics in Integrated Ocean Observing Networks: Potential for Studying Harmful Algal Blooms. In *Real-Time Observation Systems for Ecosystem Dynamicsand Harmful Algal Blooms*, page 23. UNESCO, Jan. 2007.

[63] J. A. Sethian. Fast marching methods. *SIAM review*, 41(2):199–235, 1999.

[64] B. A. Stauffer, H. A. Bowers, E. Buckley, T. W. Davis, T. H. Johengen, R. Kudela, M. A. McManus, H. Purcell, G. J. Smith, A. Vander Woude, and M. N. Tamburri. Considerations in Harmful Algal Bloom Research and Monitoring: Perspectives From a Consensus-Building Workshop and Technology Testing. *Frontiers in Marine Science*, 6, 2019. Publisher: Frontiers.

[65] D. N. Subramani, P. F. J. Lermusiaux, P. J. Haley, Jr., C. Mirabito, S. Jana, C. S. Kulkarni, A. Girard, D. Wickman, J. Edwards, and J. Smith. Time-optimal path planning: Real-time sea exercises. In *Oceans '17 MTS/IEEE Conference*, Aberdeen, June 2017.

[66] A. Thornton, T. Weinhart, O. Bokhove, B. Zhang, D. Sar, K. Kumar, M. Pisarenco, M. Rudnaya, V. Savceno, J. Rademacher, J. Zijlstra, A. Szabelska, J. Zyprych-Walczak, M. Schans, V. Timperio, and F. Veerman. Modeling and optimization of algae growth. In J. Frank, R. van der Mei, A. den Boer, J. Bosman, N. Bouman, S. van Dam, and C. Verhoef, editors, *Proceedings of the 72nd European Study Group Mathematics with Industry*, pages 54–85, Amsterdam, 2010. CWI.

[67] E. R. Twomey and R. P. Signell. Construction of a 3-arcsecond digital elevation model for the Gulf of Maine. Open-File Report 2011–1127, U.S. Geological Survey, 2013.

[68] M. P. Ueckermann and P. F. J. Lermusiaux. 2.29 Finite Volume MATLAB Framework Documentation. MSEAS Report 14, Department of Mechanical Engineering, Massachusetts Institute of Technology, Cambridge, MA, 2012.

[69] M. P. Ueckermann and P. F. J. Lermusiaux. Hybridizable discontinuous Galerkin projection methods for Navier–Stokes and Boussinesq equations. *Journal of Computational Physics*, 306:390–421, 2016.

[70] C. W. Warren. A technique for autonomous underwater vehicle route planning. *IEEE Journal of Oceanic Engineering*, 15(3):199–204, 1990.

[71] C. Yarish, J. K. Kim, S. Lindell, and H. Kite-Powell. Developing an environmentally and economically sustainable sugar kelp aquaculture industry in southern New England: from seed to market. *EEB Articles*, Nov. 2017.